Chapter 15
The ISING Model

15.1 The Model

Ferromagnetic materials are materials which develop a non-vanishing magnetization M even in the absence of an external magnetic field B. It is an experimental observation, that this magnetization decreases smoothly with increasing temperature, and vanishes above the critical temperature T_C, referred to as CURIE temperature [1]. Above this temperature the magnetization is zero and the material is no longer ferromagnetic but paramagnetic. This typical situation is illustrated in Fig. 15.1 and it is the signature of a *phase transition*. In a theoretical description of this transition the magnetization M serves as an order parameter.[1] At $T = T_C$ the system exhibits a second order phase transition: The magnetization is not differentiable with respect to T; it is, however, continuous.

The microscopic origin of this macroscopic phenomenon is based on the exchange interaction between identical particles, the atoms or molecules forming the material. The exchange interaction is a purely quantum-mechanical effect which is a consequence of the COULOMB interaction in combination with the PAULI exclusion principle.[2] For more detailed information please consult Refs. [2–8].

Given two atoms or molecules with spins S_1 and S_2, where $S_1, S_2 \in \mathbb{R}^3$, the exchange interaction energy is of the form[3]

$$E = JS_1 \cdot S_2 \ , \tag{15.1}$$

[1] For a short introduction to phase transitions in general please consult Appendix F.

[2] The statement that magnetism is a purely quantum-mechanical phenomenon that cannot explained in classical terms is known as the BOHR-VAN LEEUWEN theorem [3, 4].

[3] In this discussion we regard the spin as a classical quantity. In the quantum mechanic case one has to replace the vectors by vector operators S_i.

B.A. Stickler, E. Schachinger, *Basic Concepts in Computational Physics*,
DOI 10.1007/978-3-319-27265-8_15

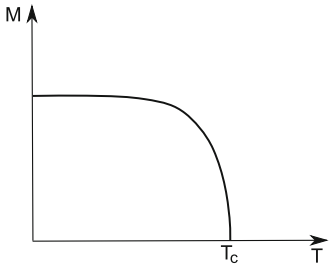

Fig. 15.1 Schematic illustration of the magnetization M as a function of temperature T in a ferromagnetic material

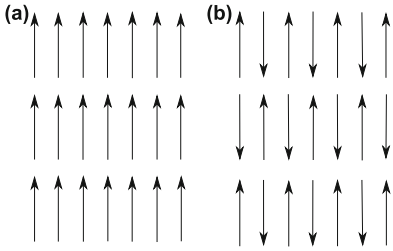

Fig. 15.2 Schematic illustration of the spin-orientation in a **(a)** ferromagnetic ($J < 0$) or **(b)** antiferromagnetic ($J > 0$) two-dimensional crystal

with the exchange constant J. The magnitude of J as well as its sign are determined by overlap integrals which include the COULOMB interaction. If $J < 0$ a parallel orientation of the spins is energetically favorable and ferromagnetism arises if $T < T_C$. On the other hand, if $J > 0$, an antiparallel orientation is established as long as the temperature does not exceed the NÉEL temperature T_N. However, in both cases the system undergoes a phase transition to a paramagnetic state if the temperature T exceeds the CURIE temperature (ferromagnetic case) or the NÉEL temperature (antiferromagnetic case). A schematic illustration of ferro- and antiferromagnetism for a two-dimensional crystal is illustrated in Fig. 15.2. We summarize the different scenarios:

$$\begin{cases} J < 0 & \text{ferromagnetic,} \\ J > 0 & \text{antiferromagnetic,} \\ J = 0 & \text{non-interacting.} \end{cases}$$

We concentrate on a cubic crystal lattice in which the atoms are localized at positions x_ℓ. The spin of atom ℓ will be denoted by $S_\ell \in \mathbb{R}^3$ and the exchange parameter between atom ℓ and atom ℓ' by $J_{\ell\ell'}$. Furthermore, we consider the ferromagnetic case with $J_{\ell\ell'} < 0$. The HAMILTON function [9–11] is of the form

$$H = \frac{1}{2} \sum_{\ell\ell'} J_{\ell\ell'} S_\ell \cdot S_{\ell'} = \frac{1}{2} \sum_{\ell\ell'} J_{\ell-\ell'} S_\ell \cdot S_{\ell'} \,. \tag{15.2}$$

Here $J_{\ell\ell'}$ was replaced by $J_{\ell-\ell'} = J_{\ell'-\ell}$ to account for translational invariance. Moreover, we define that $J_{\ell\ell} = 0$, otherwise we would have to exclude the

contributions $\ell = \ell'$ from the above sum. The HAMILTON function (15.2) is genuine to the HEISENBERG model [1]. We note that in this model there is no distinguished direction of spin orientation and, consequently, the HAMILTON function is invariant under a rotation of all spin vectors S_ℓ. The actual spin orientation may be determined by an external magnetic field or by an anisotropy of the crystal lattice. Furthermore, the restriction of the spin orientation to the positive or negative z-direction is the characteristic of the ISING model.

In a quantum mechanical description the HAMILTON operator (Hamiltonian) of the ISING model is defined by

$$H = \frac{1}{2} \sum_{\ell\ell'} J_{\ell-\ell'} S_\ell^z S_{\ell'}^z \ , \tag{15.3}$$

where S_ℓ^z are the spin operators in z-direction. If spin $1/2$ particles are described by this Hamiltonian, the spin operators S_ℓ^z are replaced by $(\hbar/2)\sigma_\ell^z$ with σ_ℓ^z the PAULI matrix and $\hbar$ the reduced PLANCK's constant. Furthermore, we redefine $J'_{\ell-\ell'} = -(\hbar^2/4)J_{\ell-\ell'}$, $J'_{\ell-\ell'} > 0$, and represent the Hamiltonian in the basis of eigenstates of the operators σ_ℓ^z. These eigenstates have eigenvalues $\sigma_\ell = \pm 1$ which correspond to *spin up* and *spin down* states, respectively. We obtain in this representation

$$H = -\frac{1}{2} \sum_{\ell\ell'} J_{\ell-\ell'} \sigma_\ell \sigma_{\ell'} - h \sum_\ell \sigma_\ell \ , \tag{15.4}$$

where we dropped the prime on the exchange parameter $J_{\ell-\ell'}$ for the sake of a more compact notation. We added, furthermore, a term which accounts for the possible coupling of the spins to an external magnetic field,[4] where h stands for the reduced field $h = -\mu_B g B/2$.[5]

There are some special cases in which the ISING model can be solved analytically [12, 13]. For instance, one can solve the general case described by Eq. (15.4) with the help of the *mean field* approximation: The contribution h_ℓ acting on site ℓ

$$h_\ell = h + \sum_{\ell'} J_{\ell-\ell'} \sigma_{\ell'} \ , \tag{15.5}$$

is replaced by its mean value

$$\langle h_\ell \rangle = h + \tilde{J} m \ , \tag{15.6}$$

[4] We note in passing that the Hamiltonian (15.4) is invariant under a spin flip of all spins if $h = 0$ ($\mathbb{Z}_2$ symmetry). This symmetry is broken if $h \neq 0$, i.e. the spins align with the external field h.

[5] We note that $H \propto \mu \cdot B$ where B is the magnetic field and μ is the magnetic moment. Furthermore, μ can be expressed as $\mu = -\mu_B g S/\hbar = -\mu_B g \sigma/2$, where μ_B is the BOHR magneton, g is the LANDÉ g-factor and σ is the vector of PAULI matrices. The sign is convention.

where $m = \langle \sigma_\ell \rangle$ and $\tilde{J} = \sum_\ell J_\ell$. (The term $\tilde{J}m$ is commonly referred to as the *molecular field*.) With the help of this ansatz it is, for instance, possible to reproduce the experimentally observed CURIE-WEISS – law of ferromagnetic materials: The temperature dependence of the magnetic susceptibility χ for $T > T_C$ can be described by:

$$\chi \propto \frac{1}{T - T_C} \,. \tag{15.7}$$

Another very interesting special case of the general model (15.4) is the restriction to nearest neighbor (n. n.) interaction with the assumption that the interaction between non-nearest neighbor spins is negligible. One step further goes the approximation that $J_{\ell-\ell'} \equiv J$ for nearest neighbors. Hence, we have

$$J_{\ell-\ell'} = \begin{cases} J & \text{if} \quad \ell, \ell' \quad \text{n. n.} \,, \\ 0 & \text{otherwise.} \end{cases} \tag{15.8}$$

In this case Eq. (15.4) is rewritten as

$$H = -\frac{J}{2} \sum_{\langle \ell\ell' \rangle} \sigma_\ell \sigma_{\ell'} - h \sum_\ell \sigma_\ell \,, \tag{15.9}$$

where $\sum_{\langle \ell\ell' \rangle}$ denotes the sum over all nearest neighbors. This model can be solved analytically in one and two dimensions if the system is assumed to be spatially unlimited. The solution in one dimension was published by E. ISING [14]. The solution in two dimensions, which is much more involved, was reported by L. ONSAGER [15].

We briefly discuss ISING's solution in one dimension. The Hamiltonian (15.9) for N-particles aligned in a one-dimensional chain is rewritten as

$$H = -J \sum_{\ell=1}^{N} \sigma_\ell \sigma_{\ell+1} - h \sum_{\ell=1}^{N} \sigma_\ell \,, \tag{15.10}$$

where we applied periodic boundary conditions, $\sigma_{N+1} = \sigma_1$, and the factor $1/2$ was absorbed into J. Let us now briefly elaborate on the kind of observables we would like to describe within this model. (We note in passing that the following discussion is not restricted to the one-dimensional case.) Given a particular spin configuration $\mathscr{C} = \{\sigma_i\}$, we assume that the probability of finding the system in this configuration

is given by the BOLTZMANN distribution $p(\mathscr{C})$[6]:

$$p(\mathscr{C}) = \frac{1}{Z_N} \exp\left[-\frac{E(\mathscr{C})}{k_B T}\right] . \tag{15.11}$$

Here, T is the temperature and k_B is BOLTZMANN's constant. The energy $E(\mathscr{C})$ associated with configuration $\mathscr{C}$ is given by Eq. (15.10). Please note that now, obviously, we have to treat the model in the classical sense, although we consider spin degrees of freedom. The partition function Z_N is given by the sum over all possible configurations $\mathscr{C}$ [3, 4, 16]:

$$Z_N = \sum_{\mathscr{C}} \exp\left[-\frac{E(\mathscr{C})}{k_B T}\right] . \tag{15.12}$$

In general, the task of solving the ISING problem is a problem of how to evaluate the sum (15.12). This is certainly not trivial since, for instance, in the one dimensional case with $N = 100$ grid-points one has $2^N = 2^{100} \approx 1.3 \times 10^{30}$ different configurations $\mathscr{C}$. On the other hand, once Z_N has been determined more information about the properties of the system can be derived [2, 12, 13]. For instance, the expectation value of the energy[7] is given by

$$\langle E \rangle = \sum_{\mathscr{C}} p(\mathscr{C}) E(\mathscr{C}) = k_B T^2 \frac{\partial}{\partial T} \ln Z_N , \tag{15.13}$$

and the expectation value of the magnetization follows from

$$\langle M \rangle = \sum_{\mathscr{C}} p(\mathscr{C}) \mathscr{M}(\mathscr{C}) = k_B T \frac{\partial}{\partial h} \ln Z_N , \tag{15.14}$$

where we defined the magnetization $\mathscr{M}(\mathscr{C})$ of a configuration $\mathscr{C}$ via:

$$\mathscr{M}(\mathscr{C}) = \left(\sum_{\ell} \sigma_\ell\right)_{\mathscr{C}} . \tag{15.15}$$

The term $\sum_\ell \sigma_\ell$ was placed within parenthesis indexed by $\mathscr{C}$ to emphasize its dependence on the particular configuration $\mathscr{C}$. From the observables (15.13) and (15.14) the *fluctuation quantities*, namely, the magnetic susceptibility, χ, and

[6] In particular we assume ergodicity of the system as will be explained in Chap. 16.

[7] $\langle E \rangle$ is also referred to as internal energy U.

the heat capacity, c_h, can be derived. The following relations hold:

$$\chi = \frac{\partial}{\partial h} \langle M \rangle \quad \text{and} \quad c_h = \frac{\partial}{\partial T} \langle E \rangle \ . \tag{15.16}$$

Equation (15.13) is applied to rewrite the expression for the heat capacity:

$$c_h = \sum_{\mathscr{C}} E(\mathscr{C}) \frac{\partial}{\partial T} p(\mathscr{C}) \ . \tag{15.17}$$

Here we made use of the fact that $E(\mathscr{C})$ is independent of temperature T. We evaluate, furthermore, the derivative of $p(\mathscr{C})$ with respect to temperature T:

$$\begin{aligned} \frac{\partial}{\partial T} p(\mathscr{C}) &= \frac{\partial}{\partial T} \left[\frac{\exp\left(-\frac{E(\mathscr{C})}{k_\mathrm{B} T}\right)}{Z_N} \right] \\ &= \frac{p(\mathscr{C})}{k_\mathrm{B} T^2} \left[E(\mathscr{C}) - \langle E \rangle \right] \ . \end{aligned} \tag{15.18}$$

This is inserted into Eq. (15.17) and results in a final expression for the heat capacity:

$$\begin{aligned} c_h &= \frac{1}{k_\mathrm{B}} T^2 \sum_{\mathscr{C}} p(\mathscr{C}) \left[E^2(\mathscr{C}) - E(\mathscr{C}) \langle E \rangle \right] \\ &= \frac{1}{k_\mathrm{B} T^2} \left(\langle E^2 \rangle - \langle E \rangle^2 \right) \\ &= \frac{1}{k_\mathrm{B} T^2} \mathrm{var}\,(E) \ . \end{aligned} \tag{15.19}$$

This result justifies why the heat capacity is referred to as a fluctuation quantity.

We determine now, following the same ideas, the magnetic susceptibility using relation (15.14):

$$\chi = \sum_{\mathscr{C}} \mathscr{M}(\mathscr{C}) \frac{\partial}{\partial h} p(\mathscr{C}) \ . \tag{15.20}$$

We note that

$$\frac{\partial}{\partial h} E(\mathscr{C}) = -\mathscr{M}(\mathscr{C}) \ , \tag{15.21}$$

and obtain:

$$\frac{\partial}{\partial h} p(\mathscr{C}) = \frac{\partial}{\partial h} \left[\frac{\exp\left(-\frac{E(\mathscr{C})}{k_\mathrm{B}T}\right)}{Z_N} \right]$$
$$= \frac{p(\mathscr{C})}{k_\mathrm{B}T} \left[\mathscr{M}(\mathscr{C}) - \langle M \rangle \right] . \tag{15.22}$$

This results in a final expression for the magnetic susceptibility χ which relates it to the variance of the magnetization M:

$$\chi = \frac{1}{k_\mathrm{B}T} \sum_{\mathscr{C}} p(\mathscr{C}) \left[\mathscr{M}^2(\mathscr{C}) - \mathscr{M}(\mathscr{C}) \langle M \rangle \right]$$
$$= \frac{1}{k_\mathrm{B}T} \left(\langle M^2 \rangle - \langle M \rangle^2 \right)$$
$$= \frac{1}{k_\mathrm{B}T} \mathrm{var}(M) . \tag{15.23}$$

After this excursion, we return to the analytic treatment of the infinite one-dimensional ISING model with nearest neighbor interaction, Eq. (15.10). If it were possible to evaluate the partition function Z_N, the required observables would be directly accessible via the above relations. In most cases this task is not analytically feasible. Nevertheless, in our particular case it appears to be possible because we recognize that we can actually evaluate Eq. (15.12) explicitly by keeping in mind Eq. (15.9):

$$Z_N = \sum_{\mathscr{C}} p(\mathscr{C})$$
$$= \sum_{\mathscr{C}} \exp\left[\frac{1}{k_\mathrm{B}T} \left(J \sum_{\ell=1}^{N} \sigma_\ell \sigma_{\ell+1} + h \sum_{\ell=1}^{N} \sigma_\ell \right) \right]$$
$$= \sum_{\mathscr{C}} \prod_{\ell=1}^{N} \exp\left[\frac{J}{k_\mathrm{B}T} \sigma_\ell \sigma_{\ell+1} + \frac{h}{2k_\mathrm{B}T} (\sigma_\ell + \sigma_{\ell+1}) \right] . \tag{15.24}$$

In the last step the sum over σ_ℓ was replaced by an alternative sum

$$\sum_{\ell=1}^{N} \sigma_\ell = \frac{1}{2} \sum_{\ell=1}^{N} (\sigma_\ell + \sigma_{\ell+1}) , \tag{15.25}$$

which is a consequence of the periodic boundary conditions $\sigma_{N+1} = \sigma_1$. Equation (15.24) can be rewritten as

$$Z_N = \mathrm{tr}\left(\mathscr{T}^N\right) , \tag{15.26}$$

where $\mathrm{tr}\,(\cdot)$ denotes the *trace* operation and we introduced the *transfer* matrix:

$$\mathscr{T}_{\sigma,\sigma'} = \exp\left[\frac{J}{k_\mathrm{B}T}\sigma\sigma' + \frac{h}{2k_\mathrm{B}T}\left(\sigma + \sigma'\right)\right] . \tag{15.27}$$

Let us briefly clarify this point: The trace operation in the basis of the spin eigenvalues $\sigma = \pm 1$ results in

$$\mathrm{tr}\,(\mathscr{T}) = \sum_\sigma \mathscr{T}_{\sigma,\sigma} = T_{-1,-1} + T_{1,1} . \tag{15.28}$$

Hence, we have

$$\begin{aligned}
\mathrm{tr}\left(\mathscr{T}^N\right) &= \sum_\sigma \left(\mathscr{T}^N\right)_{\sigma\sigma} \\
&= \sum_\sigma \sum_{\substack{\{\sigma_i\} \\ i=1,\ldots,N-1}} \mathscr{T}_{\sigma,\sigma_1}\mathscr{T}_{\sigma_1,\sigma_2}\cdots\mathscr{T}_{\sigma_{N-1},\sigma} \\
&= \sum_{\substack{\{\sigma_i\} \\ i=1,\ldots,N}} \mathscr{T}_{\sigma_1,\sigma_2}\mathscr{T}_{\sigma_2,\sigma_3}\cdots\mathscr{T}_{\sigma_N,\sigma_1} .
\end{aligned} \tag{15.29}$$

In the last step we redefined the sum indices and we used the notation $\{\sigma_i\}$ to indicate that the sum runs over all possible values of $\sigma_1, \sigma_2, \ldots, \sigma_N$ in order to abbreviate the notation. However, the sum over all possible values of $\sigma_1, \sigma_2, \ldots, \sigma_N$ can be replaced by a sum over all configurations $\mathscr{C}$ where one configuration is a specific combination of definite values $\sigma_1, \sigma_2, \ldots, \sigma_N$. For these definite values the product of transfer matrices in Eq. (15.29) is equivalent to the product of exponentials in Eq. (15.24) due to our definition of the transfer matrix $\mathscr{T}_{\sigma,\sigma'}$. Hence we demonstrated that expression (15.26) is indeed equivalent to Eq. (15.24).

It follows from definition (15.27) that

$$\mathscr{T} = \begin{pmatrix} \exp\left(\frac{J+h}{k_\mathrm{B}T}\right) & \exp\left(-\frac{J}{k_\mathrm{B}T}\right) \\ \exp\left(-\frac{J}{k_\mathrm{B}T}\right) & \exp\left(\frac{J-h}{k_\mathrm{B}T}\right) \end{pmatrix} . \tag{15.30}$$

It is an easy task to determine the eigenvalues of this matrix [17, 18]. The characteristic polynomial

$$\det \begin{pmatrix} \exp\left(\frac{J+h}{k_B T}\right) - \lambda & \exp\left(-\frac{J}{k_B T}\right) \\ \exp\left(-\frac{J}{k_B T}\right) & \exp\left(\frac{J-h}{k_B T}\right) - \lambda \end{pmatrix} \tag{15.31}$$

is of the form

$$\begin{aligned} &\left[\exp\left(\frac{J+h}{k_B T}\right) - \lambda\right]\left[\exp\left(\frac{J-h}{k_B T}\right) - \lambda\right] - \exp\left(-\frac{2J}{k_B T}\right) \\ &= \lambda^2 - 2\lambda \exp\left(\frac{J}{k_B T}\right) \cosh\left(\frac{h}{k_B T}\right) + 2\sinh\left(\frac{2J}{k_B T}\right) \\ &\stackrel{!}{=} 0 \,, \end{aligned} \tag{15.32}$$

which is easily solved. We get for the two eigenvalues $\lambda_{1,2}$

$$\begin{aligned} \lambda_{1,2} = &\exp\left(\frac{J}{k_B T}\right) \cosh\left(\frac{h}{k_B T}\right) \\ &\pm \sqrt{\exp\left(\frac{2J}{k_B T}\right) \sinh^2\left(\frac{h}{k_B T}\right) + \exp\left(-\frac{2J}{k_B T}\right)} \,, \end{aligned} \tag{15.33}$$

and note that $\lambda_1 \geq \lambda_2$ for all temperatures $T \geq 0$.

We now make use of the fact that the trace is invariant under a basis transformation Γ. Hence we can express the transfer matrix in a basis in which it is diagonal and set

$$\mathscr{T}' = \Gamma \mathscr{T} \Gamma^{-1} = \begin{pmatrix} \lambda_1 & 0 \\ 0 & \lambda_2 \end{pmatrix} \,, \tag{15.34}$$

which immediately results in:

$$Z_N = \lambda_1^N + \lambda_2^N \,. \tag{15.35}$$

Everything required to calculate the expectation value of energy *per particle* $\langle \varepsilon \rangle$

$$\langle \varepsilon \rangle = \frac{k_B T^2}{N} \frac{\partial}{\partial T} \ln Z_N \,, \tag{15.36}$$

in the *thermodynamic* limit $N \to \infty$ is now in place and, thus, we can investigate the possibility of a phase transition. First, we consider the limit

$$\lim_{N\to\infty} \frac{1}{N} Z_N = \lim_{N\to\infty} \frac{1}{N} \ln\left(\lambda_1^N + \lambda_2^N\right) = \ln \lambda_1 \ , \tag{15.37}$$

since $\lambda_1 \geq \lambda_2$ for all $T \geq 0$.[8]

If there is no external field, i.e. $h = 0$, we have

$$\lim_{N\to\infty} \frac{1}{N} Z_N = \ln\left[2\cosh\left(\frac{J}{k_B T}\right)\right] \ , \tag{15.38}$$

which is a smooth function of T for $T \geq 0$. Consequently, we do not observe a phase transition in the one dimensional ISING model. Even more information about the system can be provided by the spin correlation function $\langle \sigma_\ell \sigma_{\ell'} \rangle$

$$\langle \sigma_\ell \sigma_{\ell'} \rangle = \sum_{\mathscr{C}} p(\mathscr{C}) \sigma_\ell \sigma_{\ell'} \ . \tag{15.39}$$

A basic, however, tedious calculation shows that in the thermodynamic limit it is described by

$$\langle \sigma_\ell \sigma_{\ell'} \rangle = \left(\frac{\lambda_2}{\lambda_1}\right)^{\ell - \ell'} \ , \tag{15.40}$$

with the result that the spin correlation decreases with increasing distance $\ell - \ell'$ since $\lambda_2 < \lambda_1$ for $T > 0$.

We move on and briefly sketch the solution of the infinite two-dimensional ISING model according to L. ONSAGER [15]. The HAMILTON function (15.10) changes into:

$$H = -J \sum_{\ell\ell'} \sigma_{\ell,\ell'} \left(\sigma_{\ell+1,\ell'} + \sigma_{\ell-1,\ell'} + \sigma_{\ell,\ell'-1} + \sigma_{\ell,\ell'+1}\right) - h \sum_{\ell,\ell'} \sigma_{\ell,\ell'} \ . \tag{15.41}$$

[8] We transform

$$\lambda_1^N + \lambda_2^N = \lambda_1^N \left[1 + \left(\frac{\lambda_2}{\lambda_1}\right)^N\right] \ ,$$

and use that

$$\left(\frac{\lambda_2}{\lambda_1}\right)^N \to 0, \qquad \text{as} \qquad N \to \infty \ .$$

The strategy developed for the one-dimensional case can again be applied: The system is treated as a classical system with spin degrees of freedom. The HAMILTON function (15.41) is inserted into the expression, Eq. (15.12) for the partition function Z_N. With the help of the correct basis Z_N can be described by the trace over a product of transfer matrices. However, in this case the transfer matrix $\mathscr{T}$ is of dimension $2N \times 2N$ rather than 2×2. It is quite obvious that the search for the largest eigenvalue for arbitrary values of N is not a trivial task. Therefore, we limit our discussion to a summary of the most important results for the particular case $h = 0$.

In the two-dimensional case a phase transition is indeed observed: The magnetic susceptibility becomes singular at a particular temperature T_C. This temperature is given as the solution of equation:

$$2 \tanh^2 \left(\frac{2J}{k_B T_C} \right) = 1 \; . \tag{15.42}$$

The expectation value of the energy per particle takes on the form

$$\langle \varepsilon \rangle = -J \coth \left(\frac{2J}{k_B T} \right) \left\{ 1 + \frac{2}{\pi} K_1(\xi) \left[2 \tanh^2 \left(\frac{2J}{k_B T} \right) - 1 \right] \right\} \; , \tag{15.43}$$

where $K_1(\xi)$ is the complete elliptic integral of the first kind [see Eq. (1.14)] with the argument:

$$\xi = \frac{2 \sinh \left(\frac{2J}{k_B T} \right)}{\cosh^2 \left(\frac{2J}{k_B T} \right)} \; . \tag{15.44}$$

The magnetization per particle $\langle m \rangle$ is proved to be determined from

$$\langle m \rangle = \begin{cases} \dfrac{(1+z^2)^{\frac{1}{4}} (1 - 6z^2 + z^4)^{\frac{1}{8}}}{\sqrt{1 - z^2}} & \text{for } T < T_C \; , \\ 0 & \text{for } T > T_C \; , \end{cases} \tag{15.45}$$

with

$$z = \exp \left(-\frac{2J}{k_B T} \right) \; .$$

Equation (15.45) clearly describes a phase transition at $T = T_C$.

15.2 Numerics

We study a finite two-dimensional ISING model on a square lattice Ω with grid-points (x_i, y_j), $i,j = 1,2,\ldots,N$, which will be denoted by (i,j). We write the HAMILTON function in the form

$$H = -J \sum_{\left\langle \substack{ij \\ i'j'} \right\rangle} \sigma_{i,j}\sigma_{i',j'} - h \sum_{ij} \sigma_{i,j} \,, \tag{15.46}$$

where the $\sigma_{i,j} \in \{-1,1\}$ are treated as 'classical' spins. We consider nearest neighbor interaction and regard the exchange parameter as independent of the actual positions i,j. The problem is easily motivated: We calculate numerically observables like the expectation value of the energy or of the magnetization which will then be compared with analytic results. Such a procedure provides a rather simple check of the quality of the numerical approach which can then be extended to similar models which cannot any longer be treated analytically. We need numerical methods because summing over all possible configurations in a calculation of the partition function Z_N is simply no longer feasible since, for instance, for $N = 100$ we have $2^{N^2} = 2^{10000} \approx 10^{3000}$ possible configurations which will have to be considered as follows from Eqs. (15.12), (15.13), and (15.14). A more convenient approach would be to approximate the sums with the help of methods we encountered within the context of Monte-Carlo integration in Sect. 14.2. For instance, the estimate of the energy expectation value is given by

$$\langle E \rangle = \frac{1}{M} \sum_{i=1}^{M} E(\mathscr{C}_i) \pm \sqrt{\frac{\mathrm{var}\,(E)}{M}} \,. \tag{15.47}$$

Here, $\mathscr{C}_i$, $i = 1,2,\ldots,M$ are M configurations drawn from the pdf (15.11), the BOLTZMANN distribution. Equation (15.47) is referred to as the *estimator* of the internal energy. We note that we also have to calculate an estimate of the variance of E using a similar approach in order to determine the error induced by this approximation.[9]

Hence, there remains the task to find configurations $\mathscr{C}_i$ which follow the BOLTZMANN distribution (15.11). The inverse transformation method of Sect. 13.2 cannot be applied since $E(\mathscr{C}_i)$ is not invertible. Furthermore, the rejection method

[9] In particular $\mathrm{var}\,(E) = \langle E^2 \rangle - \langle E \rangle^2$ is to be determined and only the second term is already known. The first term, $\langle E^2 \rangle$, is then estimated with the help of

$$\langle E^2 \rangle = \frac{1}{M} \sum_{i=1}^{M} E_i^2 \,.$$

is useless since we would need the partition function Z_N to make it work. However, calculating the partition function is a task as difficult as calculating the internal energy (15.13) without any approximations. Therefore, the method of choice will be the METROPOLIS algorithm discussed in Sect. 14.3.

Let $\mathscr{C}$ be a given spin configuration on the two-dimensional square lattice Ω. We modify the spin on one particular grid-point (i,j) and obtain a *trial* spin configuration $\mathscr{C}^t$. According to our discussion in Sect. 14.3, the probability of accepting the new configuration $\mathscr{C}^t$ is then given by

$$\begin{aligned} \Pr(A|\mathscr{C}^t,\mathscr{C}) &= \min\left(\frac{p(\mathscr{C}^t)}{p(\mathscr{C})},1\right) = \min\left\{\exp\left[-\frac{E(\mathscr{C}^t)-E(\mathscr{C})}{k_{\mathrm{B}}T}\right],1\right\} \\ &= \min\left[\exp\left(-\frac{\Delta E_{ij}}{k_{\mathrm{B}}T}\right),1\right] . \end{aligned} \tag{15.48}$$

The spin orientation was changed only on one grid-point (i,j), with $\sigma_{i,j} \to \hat{\sigma}_{i,j} = -\sigma_{i,j}$; thus, the energy difference ΔE_{ij} is easily evaluated using

$$\Delta E_{ij} = 2J\sigma_{i,j}\left(\sigma_{i+1,j}+\sigma_{i-1,j}+\sigma_{i,j-1}+\sigma_{i,j+1}\right)+2h\sigma_{i,j} . \tag{15.49}$$

with $\sigma_{i,j}$ the original spin orientation.

We focus now on numerical details, some particular to the numerical treatment of the ISING model [19], and some of rather general nature which should be considered whenever a Monte-Carlo simulation is planned.

(1) Lattice Geometry

We regard a two-dimensional $N \times N$ square lattice with periodic boundary conditions[10] in order to reduce finite volume effects. It is of advantage to write a program code which will help to identify the nearest neighbors of some grid-point, since we will need this information in the METROPOLIS run whenever we calculate the energy difference due to a spin flip according to Eq. (15.49). To help with this task a matrix *neighbor*(*site*, i) will be generated only once for each choice of the system size N. Here $i = 1,2,3,4$ are the directions to the neighboring grid-points of the grid-point *site*. In a first step the sites of the square lattice are relabeled following

[10]Periodic boundary conditions in two dimensions imply that

$$\sigma_{N+1,j} = \sigma_{1,j} \qquad \text{and} \qquad \sigma_{i,N+1} = \sigma_{i,1} ,$$

for all i,j.

the scheme[11]:

$$\begin{array}{cc} N(N-1)+1 & \cdots N^2 \\ \vdots & \vdots \quad \vdots \\ N+1 & \cdots 2N \\ 1 & 2 \cdots N\,. \end{array} \tag{15.50}$$

In the next step, the matrix *neighbor* is initialized as an array of size $N^2 \times 4$. Every *site* has four nearest neighbors: *up*, *right*, *down*, and *left*. The corresponding matrix elements for periodic boundary conditions can be evaluated according to the following scheme:

- For *up* we have:
  (a) If $site + N \leq N^2$: $up = site + N$,
  (b) else if $site + N > N^2$: $up = site - N(N-1)$.
- For *right* we have:
  (a) If $\mathrm{mod}(site, N) \neq 0$: $right = site + 1$,
  (b) else if $\mathrm{mod}(site, N) = 0$: $right = site - N + 1$.
- For *down* we have:
  (a) If $site - N \geq 1$: $down = site - N$,
  (b) else if $site - N < 1$: $down = site + N(N-1)$
- For *left* we have:
  (a) If $\mathrm{mod}(site - 1, N) \neq 0$: $left = site - 1$,
  (b) else if $\mathrm{mod}(site - 1, N) = 0$: $left = site + N - 1$.

In a final step, the array elements are rearranged according to

$$neighbor(site, :) = [up, right, down, left]\,, \tag{15.51}$$

where $site = 1, 2, \ldots, N^2$.

(2) Initialization

It has already been discussed in Sect. 14.3 that the quality of random numbers generated with the help of the METROPOLIS algorithm is highly dependent on the choice of initial conditions. This is, in our case, the initial spin configuration $\mathscr{C}_0$.

[11] In the following we will refer to the notation (i), $i = 1, 2, \ldots, N^2$ as the *single-index* notation while the notation (i, j), $i, j = 1, 2, \ldots, N$ will be referred to as the *double-index* notation.

Of course, it would be favorable to start with a configuration which was already drawn from the BOLTZMANN distribution $p(\mathscr{C})$. However, in practice this is not feasible ab initio. But, as will be elucidated in Chap. 16, the METROPOLIS algorithm produces configurations which become independent of the initial state and follow the BOLTZMANN distribution. Hence we can simply start with some arbitrary configuration and discard it together with the first n constituents of the sequence $\mathscr{C}_0, \mathscr{C}_1, \ldots, \mathscr{C}_n$. This method is referred to as *thermalization*.[12] The question arises: can n be determined to ensure that the sequence starting with $\mathscr{C}_{n+1}$ will conform to the pdf $p(\mathscr{C})$?

There are two different ways to approach this problem: (i) The first is to measure auto-correlations between configurations $\mathscr{C}_i$ where it has to be ensured that the set of states is sufficiently large to allow for a significant conclusion. We will discuss auto-correlations in more detail in Chap. 19. (ii) The second approach is to empirically check whether equilibrium has been reached or not. For instance, one could simply plot some selected observables and check when the initial bias vanishes. In this case the observable reaches some saturation value as a function of the number of measurements. A particularly useful method is to start the algorithm with at least two different configurations. As soon as equilibrium has been reached, the observables should approach the same saturation values after a certain (finite) number of measurements. Typical choices are the *cold start* and the *hot start*. Cold start means that the temperature is initially below the critical temperature, i.e. in the ISING model all spins are aligned (ferromagnetic state). Hot start means that the temperature is well above the critical temperature and for the ISING model the spin orientation is chosen at random for any site (paramagnetic state).

(3) Execution of the Code

The METROPOLIS algorithm for the ISING model is executed in the following steps:

1. Choose an initial configuration $\mathscr{C}_0$.
2. We migrate through the lattice sites systematically.[13] Suppose we just reached site (i,j) (we use the double-index notation $i,j = 1,2,\ldots,N$, to improve the readability) and our current configuration is $\mathscr{C}_k$. Then k configurations have been accepted so far. We generate a new configuration $\mathscr{C}^t$ from $\mathscr{C}_k$ by replacing in $\mathscr{C}_k$ the entry $\sigma_{i,j}$ by $-\sigma_{i,j}$.

[12] The number of configurations discarded is referred to as the thermalization length.

[13] A migration through all lattice sites is referred to as a *sweep*.

3. The new configuration is accepted with probability

$$\Pr(A|\mathscr{C}^t, \mathscr{C}_k) = \min\left[\exp\left(-\frac{\Delta E_{ij}}{k_B T}\right), 1\right] , \tag{15.52}$$

   where ΔE_{ij} is determined from Eq. (15.49). $\mathscr{C}^t$ is accepted if $\Pr(A|\mathscr{C}^t, \mathscr{C}_k)$ is equal to one or if $\Pr(A|\mathscr{C}^t, \mathscr{C}_k) \geq r \in [0, 1]$ otherwise $\mathscr{C}^t$ is rejected. If $\mathscr{C}^t$ was accepted we set $\mathscr{C}_{k+1} = \mathscr{C}^t$.
4. Go to the next lattice site [step 2].

We note that instead of sampling the lattice sites sequentially as suggested in step 2 the lattice sites can also be sampled randomly with the help of

$$i = \text{int}(rN^2) + 1 , \tag{15.53}$$

where $r \in [0, 1]$ is a uniformly distributed random number and $\text{int}(\cdot)$ denotes the integer part of a given quantity. Obviously, Eq. (15.53) is only useful in the single-index notation $i = 1, 2, \ldots, N^2$.

(4) Measurement

As soon as thermalization was achieved the procedure to measure interesting observables can be started. Such a procedure consists of collecting the data required and in calculating expectation values as was illustrated in Eq. (15.47) for the case of the expectation value of the energy. A more detailed study of estimator techniques is postponed to Chap. 19. However, there is one crucial point one should be aware of: We already mentioned in our discussion of the METROPOLIS algorithm in Sect. 14.3 that subsequent configurations $\mathscr{C}_k$ may be strongly correlated. This problem can be circumvented by simply neglecting intermediate configurations. For instance, one may allow a couple of 'empty' sweeps between two measurements.

In the following we discuss some selected results obtained with the numerical approach described above.

15.3 Selected Results

We investigate the two-dimensional ISING model with periodic boundary conditions and we chose $h = 0$ and $J = 0.5$ for all following illustrations.

In a first experiment we plan to check the thermalization process and, thus, measure after every single sampling step and skip thermalization. The observables of interest, the expectation value of the energy per particle, $\langle\varepsilon\rangle$, and the expectation value of the magnetization per particle, $\langle m\rangle$, are illustrated in Fig. 15.3 for 30 sweeps

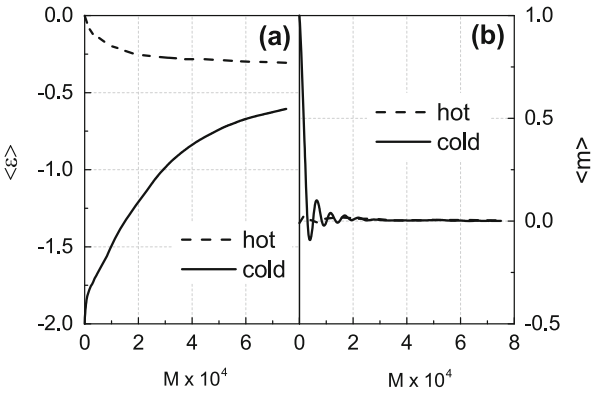

Fig. 15.3 Time evolution of **(a)** the expectation value of the energy per particle $\langle \varepsilon \rangle$ and **(b)** of the expectation value of the magnetization per particle $\langle m \rangle$ vs the number of measurements M. We used a cold start (*solid line*) and a hot start (*dashed line*) to achieve these results

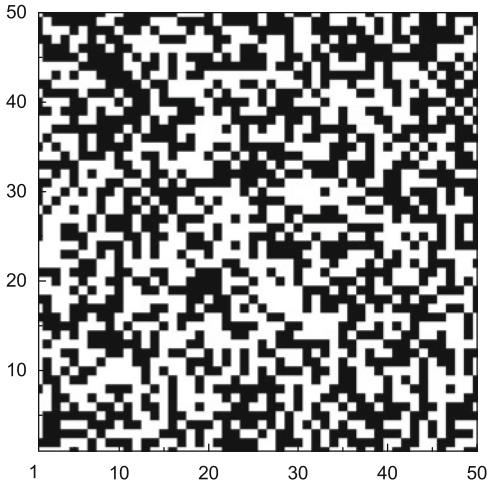

Fig. 15.4 Typical spin configuration for a temperature well above the critical temperature T_C. *Black shaded areas* correspond to spin up sites while the *white areas* are spin down sites

in a system of the size $N = 50$ which corresponds to $m \sim 8 \times 10^4$ measurements. Moreover, we set $k_B T = 3$ which should be well above T_C according to Eq. (15.42). Hence, we expect paramagnetic behavior, i.e. $\langle m \rangle = 0$ in the equilibrium since the acceptance probability is rather large because the spins are randomly orientated. In addition, Fig. 15.4 shows a typical spin configuration for a temperature well above T_C.

According to Fig. 15.3b the expectation value of the magnetization per particle $\langle m \rangle$ approaches indeed zero after a rather short thermalization period independent of the starting procedure. This is certainly not the case for the energy expectation value per particle $\langle \varepsilon \rangle$, Fig. 15.3a, which does not approach saturation even after $M \sim 8 \times 10^4$ measurements for both starting procedures. The consequence is that the thermalization period certainly needs to be longer than only 30 sweeps.

Keeping this result in mind we move on to perform the next check of our numerics, namely to study the influence of the system size N on the numerical results we get for the observables $\langle\varepsilon\rangle$, $\langle m\rangle$ as well as c_h and χ as functions of temperature T. Let us outline the strategy: a thermalization period of 500 sweeps will be used and 10 sweeps between each measurement will be discarded. Moreover, we start with the *hot start* configuration and at a temperature $k_B T_0 = 3$ well above T_C. After the measurements at T_0 have been finished, the temperature is slightly decreased, $T_1 < T_0$.

One more point should be addressed: We perform a simulation using the strategy outlined above and obtain as a result some observable O as a function of temperatures $\{T_n\}$, with T_0 the initial temperature well above T_C and $T_{n+1} < T_n$. From the physics point of view, this temperature dependence will, of course, be most interesting for temperatures $T \approx T_C$. Thus, what we need is an adaptive cooling strategy designed in such a way that the temperature is decreased rapidly for temperatures $T \gg T_C$ or $T \ll T_C$, but for $T \approx T_C$ the temperature is modified only minimally. [This question will also be a very important point in the discussion of *simulated annealing*, a stochastic optimization strategy (see Sect. 20.3).] At the moment we are satisfied with equally spaced temperatures, i.e. $T_{k+1} = T_k - \delta$, where $\delta = \text{const}$ because we are mainly interested to study the influence of the system size N on our calculations.

The error bars of the calculated expectation values have been obtained with the help of Eq. (15.47). The error estimates for the heat capacity c_h as well as for the magnetic susceptibility χ are more complex to evaluate. The method employed is referred to as *statistical bootstrap*, where $M = 100$ samples have been generated. This method will be explained in some detail in Chap. 19.

In Fig. 15.5 we compare the expectation value of the energy per particle, $\langle\varepsilon\rangle$, the absolute value of the magnetization per particle $|\langle m\rangle|$, the overall heat capacity c_h and the overall magnetic susceptibility χ for four system sizes $N = 5, 20, 50, 100$. Furthermore, in Fig. 15.6 we show the curves for the system size of $N = 50$ together with corresponding error bars.

We observe that the phase transition becomes sharper with increasing system size. In fact we know, that the phase transition is infinitely sharp as $N \to \infty$ from the analytic solution given by ONSAGER. It is a quite obvious result of this study that the system size N should be greater than 20 to achieve acceptable results.

Furthermore, we presented the absolute value of the magnetization rather than the magnetization itself. The reason is that for $T < T_C$ the ground state is degenerate. In particular, the state with all spins up or all spins down is equally probable since we set the external magnetic field $h = 0$. This is a manifestation of the $\mathbb{Z}_2$ symmetry of the Hamiltonian discussed in Sect. 15.1.

Of particular interest is the region around the critical temperature, referred to as the *critical region*. In this region, the spins are not perfectly aligned and not randomly orientated either. In this region the spins align in so called *magnetic domains*, which are also referred to as WEISS domains [1]. A typical spin configuration which exhibits such domains is presented in Fig. 15.7.

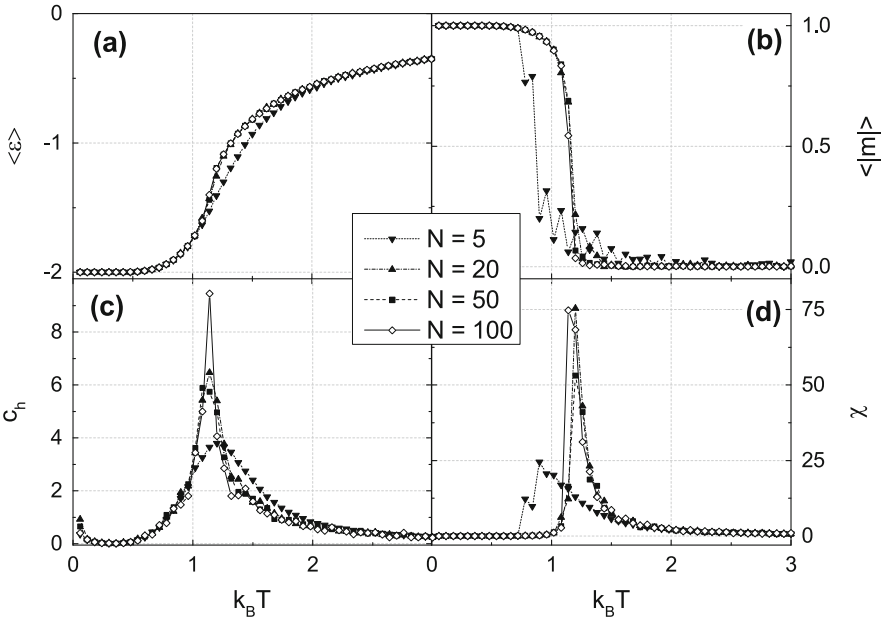

Fig. 15.5 **(a)** The expectation value of the energy per particle $\langle\varepsilon\rangle$, **(b)** the absolute value of the expectation value of the magnetization per particle $|\langle m\rangle|$, **(c)** the heat capacity c_h, and **(d)** the magnetic susceptibility χ vs temperature $k_B T$ for the two-dimensional ISING model. The system sizes are $N = 5, 20, 50, 100$

We conclude this chapter with an interesting note: Fig. 15.6 makes it quite clear that the error of the expectation value of the magnetization and of the energy is biggest for values around the transition temperature. In fact, if we increase the system size the error will become even larger. The reason is quite obvious: The error of our Monte-Carlo integration is proportional to the square root of the variance of the investigated observable. However, since we deal with a second order phase transition, this variance tends to infinity as $N \to \infty$ [4]. There is one cure to the problem: We are dealing here with finite-sized systems, thus, the variance will never actually be infinitely large. Furthermore, according to Eq. (15.47) we can decrease the error by increasing the number of measurements. Hence, if one is confronted with large systems, one has also to perform many measurements in order to reduce the error.[14]

[14]We note from Eq. (15.47) that we have to perform four times as many measurements in order to reduce the error by a factor 2.

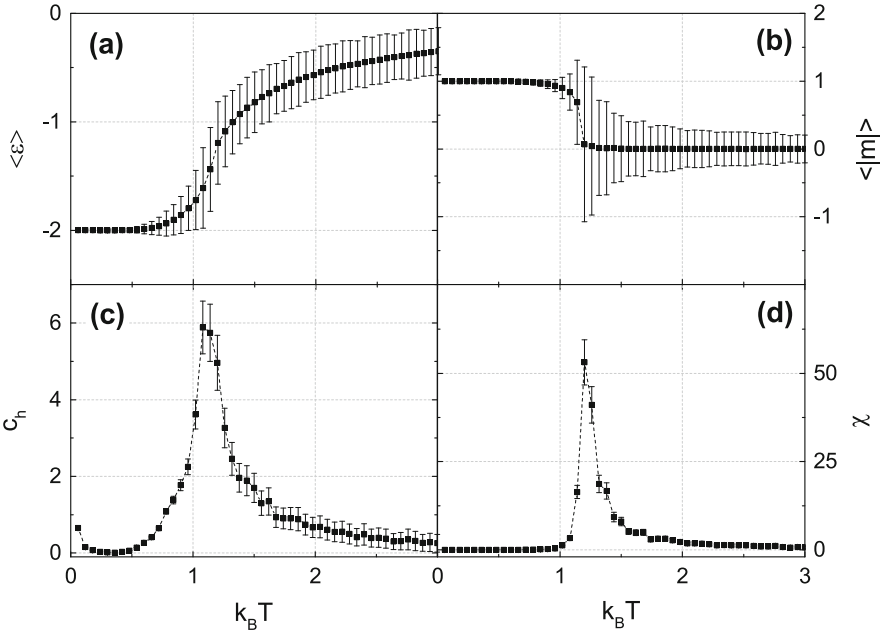

Fig. 15.6 **(a)** The expectation value of the energy per particle $\langle\varepsilon\rangle$, **(b)** the expectation value of the magnetization per particle $|\langle m\rangle|$, **(c)** the heat capacity c_h, and **(d)** the magnetic susceptibility χ with error bars vs temperature $k_B T$ obtained for the two-dimensional ISING model of size $N = 50$

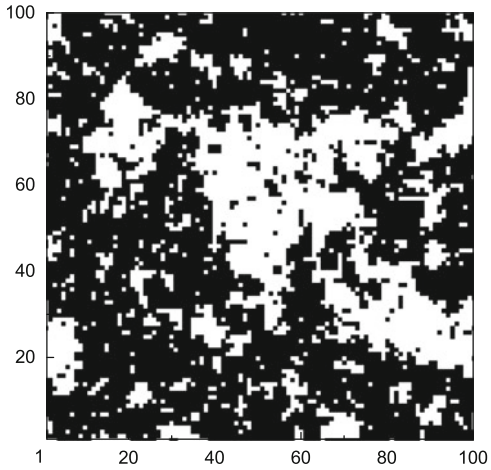

Fig. 15.7 For $T \approx T_C$ the spins organize in WEISS domains. Here we show a typical spin configuration for $N = 100$ and $k_B T = 1.15$. The *black shaded areas* correspond to spin up sites while the *white areas* indicate spin down sites

Summary

The ISING model is a rather simple model which describes effectively a second order phase transition. Such phase transitions are the topic of extensive numerical studies and, therefore, this model served here as a tool to demonstrate how to proceed from the problem analysis to a numerical algorithm which will allow to simulate the physics. The advantage of the ISING model was that under certain simplifications solutions could be derived analytically. In the course of this analysis the important concept of observables was introduced. Observables are certain physical properties of a system which characterize the specific phenomenon of interest. Numerically, observables are certain variables which are to be 'measured' within the course of a simulation. After the extensive analysis of the ISING model the transition to the numerical analysis of the two-dimensional ISING model was a rather easy part. The required modification of spin configurations turned out to be the key element of the simulation and this suggested the application of the METROPOLIS algorithm for sampling. Finally, important problems like initialization of the simulation, thermalization, finite size effects, measurement of observables, and the prevention of correlations between subsequent spin configurations caused by the METROPOLIS algorithm have been discussed on the basis of concrete calculations. The first part of this chapter was motivated by W. S. DORN and D. D. MCCRACKEN [20]:

> Numerical methods are no excuse for poor analysis.

Problems

1. Write a program to simulate the two-dimensional ISING model with periodic boundary conditions with the help of the METROPOLIS algorithm. Follow the strategy outlined in Sect. 15.2 and try to reproduce the results illustrated in Sect. 15.3 for $N = 5, 20, 50$.

   In particular, as a first step write a routine which stores the nearest neighbors of the square lattice in an array. As a second step, write a program which performs a sweep through the lattice geometry. You can either choose the lattice sites systematically or at random. As a third step, set up the main program which calls the sweep routine. Choose some initial configuration and thermalize the system. Measure the expectation value of the energy per particle as well as the absolute value of the expectation value of the magnetization for different temperatures $k_B T$ and determine the respective errors, see Eq. (15.47). Calculate also the overall magnetic susceptibility and the overall heat capacity. The determination of the error is more complicated in this case and can therefore be neglected for the moment.

   Good parameters to start with are $J = 0.5$, $N_{therm} = 500$, $N_{skip} = 10$ and $h = 0.0$.
2. Try also different values of J and $h \neq 0$.

References

1. White, R.M.: Quantum Theory of Magnetism, 3rd edn. Springer Series in Solid-State Sciences. Springer, Berlin/Heidelberg (2007)
2. Landau, L.D., Lifshitz, E.M.: Course of Theoretical Physics. Statistical Physics, vol. 5. Pergamon Press, London (1963)
3. Halley, J.W.: Statistical Mechanics. Cambridge University Press, Cambridge (2006)
4. Pathria, R.K., Beale, P.D.: Statistical Mechanics, 3rd edn. Academic, San Diego (2011)
5. Baym, G.: Lectures on Quantum Mechanics. Lecture Notes and Supplements in Physics. The Benjamin/Cummings, London/Amsterdam (1969)
6. Cohen-Tannoudji, C., Diu, B., Laloë, F.: Quantum Mechanics, vol. I. Wiley, New York (1977)
7. Sakurai, J.J.: Modern Quantum Mechanics. Addison-Wesley, Menlo Park (1985)
8. Ballentine, L.E.: Quantum Mechanics. World Scientific, Hackensack (1998)
9. Arnol'd, V.I.: Mathematical Methods of Classical Mechanics, 2nd edn. Graduate Texts in Mathematics, vol. 60. Springer, Berlin/Heidelberg (1989)
10. Goldstein, H., Poole, C., Safko, J.: Classical Mechanics, 3rd edn. Addison-Wesley, Menlo Park (2013)
11. Scheck, F.: Mechanics, 5th edn. Springer, Berlin/Heidelberg (2010)
12. Mandl, F.: Statistical Physics, 2nd edn. Wiley, New York (1988)
13. Schwabl, F.: Statistical Mechanics. Advanced Texts in Physics. Springer, Berlin/Heidelberg (2006)
14. Ising, E.: Beitrag zur Theorie des Ferromagnetismus. Z. Phys. **31**, 253 (1925)
15. Onsager, L.: Crystal statistics, I. A two-dimensional model with an order-disorder transition. Phys. Rev. **65**, 117–149 (1944). doi:10.1103/PhysRev.65.117
16. Hardy, R.J., Binek, C.: Thermodynamics and Statistical Mechanics: An Integrated Approach. Wiley, New York (2014)
17. Kwak, J.H., Hong, S.: Linear Algebra. Springer, Berlin/Heidelberg (2004)
18. Strang, G.: Introduction to Linear Algebra, 4th edn. Cambridge University Press, Cambridge (2009)
19. Stauffer, D., Hehl, F.W., Ito, N., Winkelmann, V., Zabolitzky, J.G.: Computer Simulation and Computer Algebra, pp. 79–84. Springer, Berlin/Heidelberg (1993)
20. Dorn, W.S., McCracken, D.D.: Numerical Methods with Fortran IV Case Studies. Wiley, New York (1972)